

A New Predicting Method for Long-Term Photovoltaic Storage Using Rescaled Range Analysis: Application to Two Algerian Sites

Samia Harrouni

Received: 11 October 2011 / Accepted: 27 March 2012 / Published online: 13 April 2012
© Springer Science+Business Media B.V. 2012

Abstract A new predicting approach of long-term storage capacity for autonomous PV installations has been developed using the rescaled range analysis (R/S). The method consists mainly in establishing a mathematical law between the $(R/S)_\tau$ ratio and the time period τ . The method has been tested over one year for two autonomous PV systems located in the huge desert of Algeria. Data used are converted solar energy which are not stationary. The experimental results show that even if the condition of stationarity is not satisfied, the rescaled range is well described by a power function of the time, this is possible by introducing a new exponent E . Using the power law the PV storage capacity is predicted for periods ranging from 1 to 5 years. The obtained results show that for an energy demand equalling the mean of converted energy, a storage of several months is needed to obtain the autonomy of the PV systems, consequently it will be too expensive to set-up such PV installations. Thus, an optimization method has been proposed to reduce the size of the storage. Application of this method for the two studied systems has led to significant reduction of the PV storage size.

Keywords Solar irradiation · Photovoltaic storage · Fractal · Hurst · Rescaled range analysis · Prediction

1 Introduction

Several countries have started to exploit photovoltaic energy as part of their future energy supply. To ensure the growth of the PV sector, it is necessary to deliver secure and reliable power without discontinuous while managing uncertainties related to

S. Harrouni (✉)
Instrumentation Laboratory, Faculty of Electronics and Computer,
University of Science and Technology H. Boumediene (USTHB),
P.O. Box 32, El-Alia, 16111, Algiers, Algeria
e-mail: sharrouni@yahoo.fr

fluctuations of the energy source. In fact, a fundamental characteristic of a photovoltaic system is that power is produced only while sunlight is available. Therefore, stand-alone photovoltaic generators (systems in which the photovoltaic is the sole generation source) require an electricity storage system to deliver a quasi-continuous energy supply regardless of insolation sequences.

Storage, in a photovoltaic system, accounts for a far from negligible contribution to overall operating costs, owing to successive replacements, over the system's lifetime. Indeed, overall storage cost is not subject to any downward trend, matching that achieved for the other components of photovoltaic systems.

Because of large impact of the storage system in a stand-alone photovoltaic installation, the storage sizing is one of the important questions investigated to improve the efficiency of the operation of photovoltaic systems and reduce their costs.

Several approaches have been established in order to find the best way for evaluating and predicting suitable size of the storage capacity for autonomous PV systems [1–7]. In this paper a new approach for predicting the long-term photovoltaic storage is presented. The approach is based on the statistical method: the rescaled range analysis (R/S analysis).

The paper is organized as follows: Section 2 provides a description of the rescaled range analysis. In Section 3, we present the Hurst exponent and the fractal dimension, the relation between the two parameters is also discussed, in this section the “Rectangular Covering Method” we already developed for estimating the fractal dimension of signals is also described. In Section 4, we apply the rescaled range analysis to predict the photovoltaic storage. Thus, the data bank used and the obtained results are presented in this section. Section 5 deals with the optimisation of the proposed approach. Finally in Section 6 we give a conclusion summarising our findings and results.

2 Rescaled Range Analysis

R/S analysis was established by the hydrologist Hurst in 1951 and the same was further developed by Mandelbrot and Van Ness (1968). Hurst devoted his researches to the study of the hydrology of the Nile River, in particular he was interested to the yearly changes in water level in order to adapt the dam's storage capacity according to the natural environment. Hurst observed that flood occurrences could be characterized as persistent, i.e. heavier floods were accompanied by above average flood occurrences, while below average occurrences were followed by minor floods. In the process of this finding he invented a new statistical method—the rescaled range analysis (R/S analysis)—which he described in detail in an interesting book [8].

He tried to find out the ideal features for reservoir design. An ideal reservoir should discharge certain amount of water every year and should never overflow. However, the inflow of the reservoir varies due to changes in the climatic conditions. If the inflow of the reservoir is too low then releasing fixed amount of water will make reservoir dry. Thus, he was confounded with the problem of fixing the water discharge policy, such that the reservoir will never be emptied nor it will overflow [9]. In developing such a model, Hurst studied the inflow of water from rainfall. He measured how reservoir level rises and falls around its average and recorded range of the variations.

The description of the rescaled range statistic given in the following borrows heavily from Jens Feder’s book Fractals [10].

In any given year, t , the ideal reservoir will accept the influx $\varepsilon(t)$ from the Lake (Lake Albert taken as an example by Hurst), and a volume per year (discharge), $\langle \varepsilon \rangle_\tau$, will be released from the reservoir. The average influx over the time period of τ years is:

$$\langle \varepsilon \rangle_\tau = \frac{1}{\tau} \sum_{t=1}^{\tau} \varepsilon(t) \tag{1}$$

Let $X(t)$ be the accumulated departure of the influx $\varepsilon(t)$ from the mean $\langle \varepsilon \rangle_\tau$:

$$X(t, \tau) = \sum_{u=1}^t \{ \varepsilon(u) - \langle \varepsilon \rangle_\tau \}, \quad t = 1, 2, \dots, \tau \tag{2}$$

The difference between the maximum and the minimum accumulated influx X over the time period τ is the range $R(\tau)$. This range represents the storage capacity required to maintain the mean discharge throughout the period. Thus, for an ideal reservoir, R represents the difference between the maximum and minimum amounts of water contained in the reservoir. The expression of R is:

$$R(\tau) = \max_{1 \leq t \leq \tau} X(t, \tau) - \min_{1 \leq t \leq \tau} X(t, \tau) \tag{3}$$

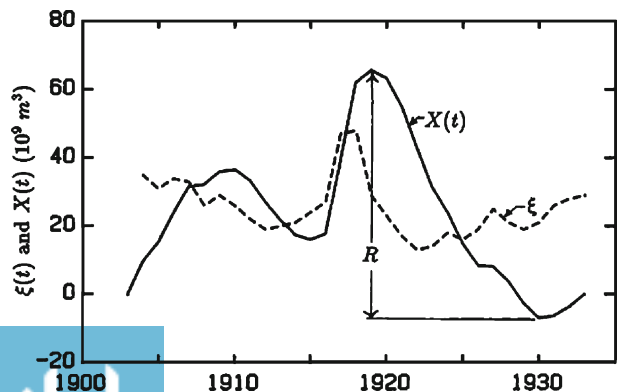
This is illustrated in Fig. 1 where the range R for the lake Albert is calculated for the first 30 years.

Clearly, we note that the range R depends on the time period τ considered and it increases with increasing τ .

In order to compare observed ranges of various phenomena, Hurst used the rescaled range R/S which is a dimensionless ratio, it is obtained by dividing the range $R(\tau)$ by the standard deviation $S(\tau)$ defined by:

$$S = \sqrt{\frac{1}{\tau} \sum_{t=1}^{\tau} \{ \varepsilon(t) - \langle \varepsilon \rangle_\tau \}^2} \tag{4}$$

Fig. 1 Lake Albert accumulated departures from the mean discharge $X(t)$ for the first 30 years. The range is indicated by R [6]



For large τ the mean value of $(R/S)_\tau$ ratio is a power function of τ :

$$(R/S)_\tau = (a\tau)^H \quad (5)$$

where a is a constant and H is the Hurst exponent. H can be estimated as the slope of the log/log plot of $(R/S)_\tau$ vs. τ by using least-squares estimation:

$$\log (R/S)_\tau = H \log \tau + \text{constant} \quad (6)$$

3 Hurst Exponent and Fractal Dimension

According to the R/S analysis theory the slope of regression line is identified to the Hurst exponent which is an index of the long memory of the time series. The Hurst exponent taking values from 0 to 1 allows the measure of the time series persistence. When $H = 1/2$ the process does not possess long memory (has independent increments), a value $1/2 < H < 1$ means that the process is persistent (positive dependent), $0 < H < 1/2$ means antipersistence (negative dependent) of the process.

The Hurst exponent is directly related to the fractal dimension of a process, which gives a measure of the roughness of the process by the relation:

$$D = 2 - H \quad (7)$$

For a curve, fractal dimension is between 1 and 2, it approaches 2 if it is extremely irregular and tends towards 1 if it is more regular.

To estimate the fractal dimension of curves, several methods exist. The most popular ones are the Box-Counting and the Minkowski–Bouligand methods. However, experimental results published in the literature showed that these two techniques suffer from inaccuracy and uncertainty. Indeed, according to [11] the precision of these estimators are mainly related to the following aspects:

- Real Value of the Fractal Dimension D : With big values of D , the estimation error is always very high. This can be explained by the effect of resolution. When the value of D increases, its estimates can not reflect the roughness of the object and higher resolution is then needed.
- Resolution: In the case of the temporal curves, the resolution consists of observation size of the curve (minute, hour, day...). Estimated fractal dimension decreases with the step of observation. This is due to the fact that a curve tends to become a horizontal line segment and appears more regular. Inversely, estimated fractal dimension tends to increase with the increase of the step of observation because, a curve tends to series of vertical line segments and appears then more irregular.
- Effect of Theoretical Approximations: Imprecision of the Box-counting and the Minkowski–Bouligand methods is also related to constraints occurring in theoretical approximations of these estimators. For example, the Box-counting dimension causes Jumps on the log–log plots which generates dispersion of the

- Choice of the Interval through which the line of the log–log plots is adjusted.

Inspired by the Minkowski–Bouligand method, a class of approaches to compute the fractal dimension of signal curves or one-dimensional profiles called covering methods is then proposed by several researchers [12–14].

These methods consist in creating multiscale covers around the signal’s graph. Indeed, each covering is formed by the union of specified structuring elements. In the method of Box–counting, the structuring element used is the square or limp, that of Minkowski–Bouligand uses the disk.

To improve the complexity and the precision of the fractal dimension estimation of time series, we have developed a new method called Rectangular covering Method [15–18].

The method consists in covering the curve for which we want to estimate fractal dimension by rectangles instead of disks like in Minkowski–Bouligand approach. The choice of this type of structuring element is due to the discrete character of the studied signals. Thus, the rectangle allows combining every point on the x-axis with the corresponding point on the y-axis, thus achieving the covering of the signal without information loss.

From the mathematical point of view, the use of the rectangle as structuring element for the covering is justified. Indeed, in [19] Bouligand showed that the Minkowski–Bouligand dimension can be obtained by also replacing the disks in the previous covers with any other arbitrarily shaped compact sets that possess a nonzero minimum and maximum distance from their centre to their boundary.

Thus, as shown in Fig. 2, for different time intervals $\Delta\tau$ the area $A(\Delta\tau)$ of this covered curve is calculated by using the following relation:

$$A(\Delta\tau) = \sum_{t_n=0}^{n-1} \Delta\tau \cdot |f(t_n + \Delta\tau) - f(t_n)| \tag{8}$$

N denotes the signal length (number of samples of the considered signal), $f(t_n)$ is the value of the function representing the signal at the time t_n and $|f(t_n + \Delta\tau) - f(t_n)|$ is the function variation related to the interval $\Delta\tau$. Bouligand defined the fractal dimension D as follows [19]:

$$D = 2 - \lambda(A) \tag{9}$$

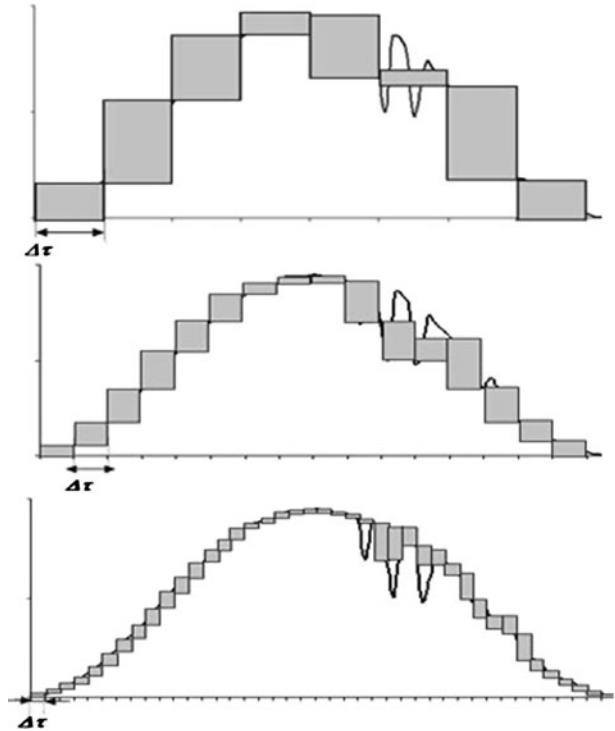
where $\lambda(A)$ is the similitude factor and it represents the infinitesimal order of $A(\Delta\tau)$. It is defined by:

$$\lambda(A) = \lim_{\Delta\tau \rightarrow 0} \frac{\log(A(\Delta\tau))}{\log(\Delta\tau)} \tag{10}$$

Replacing $\lambda(A)$ by its value in Eq. 10 we obtain:

$$D = \lim_{\Delta\tau \rightarrow 0} \left[2 - \frac{\log(A(\Delta\tau))}{\log(\Delta\tau)} \right] \tag{11}$$

Fig. 2 An example of a curve covered by rectangles at different scales $\Delta\tau$



The properties of the logarithm permit us to put Eq. 11 under the following shape:

$$D = \lim_{\Delta\tau \rightarrow 0} \left[\frac{\log \left(\frac{A(\Delta\tau)}{\Delta\tau^2} \right)}{\log \left(\frac{1}{\Delta\tau} \right)} \right] \quad (12)$$

The fractal dimension is then deduced from the following relation by using the least-squares estimation:

$$\log \left(\frac{A(\Delta\tau)}{\Delta\tau^2} \right) \cong D \cdot \log \left(\frac{1}{\Delta\tau} \right) + \text{constant} \quad (13)$$

4 New Approach for Predicting Photovoltaic Storage

4.1 Methodology

The storage predicting method proposed in this paper is based on the R/S analysis described above. In this method the PV storage (batteries) is assimilated to the water reservoir studied by Hurst. Hence, the determination of the ideal PV storage capacity size requires the estimation of the energy deficit which represents the difference between solar radiation input and energy demand on long-term period.

For a given day, d , the PV installation will accept a global irradiation $I(d)$, the PV generator will then convert this energy in $E_g(d)$ according to equation below:

$$E_g(d) = \eta(d) I(d) A_{pv} \tag{14}$$

In this relation, A_{pv} is the PV generator area, $\eta(d)$ is the daily efficiency of the PV generator.

Energy supplied by the installation to the load is assumed to be the mean converted energy $\langle E_g \rangle_\tau$ for the studied period τ . It is expressed as:

$$\langle E_g \rangle_\tau = \frac{1}{\tau} \sum_{t=1}^{\tau} E_g(t) \tag{15}$$

The accumulated difference between the converted energy and the energy demand for τ days is expressed as:

$$D(t, \tau) = \sum_{u=1}^t \{ E_g(u) - \langle E_g \rangle_\tau \} \tag{16}$$

The difference between the maximum and the minimum accumulated energy $D(t, \tau)$ is the range $R(\tau)$ which can be identified to the maximum size of PV energy storage.

$$R(\tau) = \max_{1 \leq t \leq \tau} D(t, \tau) - \min_{1 \leq t \leq \tau} D(t, \tau) \tag{17}$$

According to the Hurst empirical law equation (Eq. 5) we can take the logarithm of both the sides of the equation, we then obtain:

$$\log(R/S)_\tau = H \log \tau + H \log a \tag{18}$$

Using the least-squares estimation to fit Eq. 18 we obtain the estimation values of H and a . Knowing these parameters, one can predict the possible future value of the adjusted range $(R/S)_n$ for any period n .

To estimate the range $(R)_n$ the adjusted range must be multiplied by the standard deviation $(S)_n$. This latter is taken to be equal to the greatest value of S over the period.

4.2 Data Bank

The data used to implement this method are daily global irradiation $I(d)$ computed by integrating the global irradiance data measured at two south Algerian sites: Tahifet located in Tamanrasset (latitude = 22°53' north, longitude = 6° east and altitude = 1400 m) and Imehrou located in Illizi (latitude = 26°00' north, longitude = 8°50' east and altitude = 600 m).

The global irradiances are recorded from the operation of two 720 Wp stand-alone photovoltaic power installations during 1992-year on a 10°-tilted surface with a time step of 10 min. These systems have been installed by the National Company from Electricity and Gaz (SONELGAZ). Figure 3 gives histograms of the global irradiations used for both studied sites.

To implement our approach daily converted energies are needed, these data can be calculated according to Eq. 7. In our case the daily converted energy data are provided by monitoring the PV systems with a data acquisition. Figure 4 shows annual evolution of the monthly mean of daily converted energy E_g used.

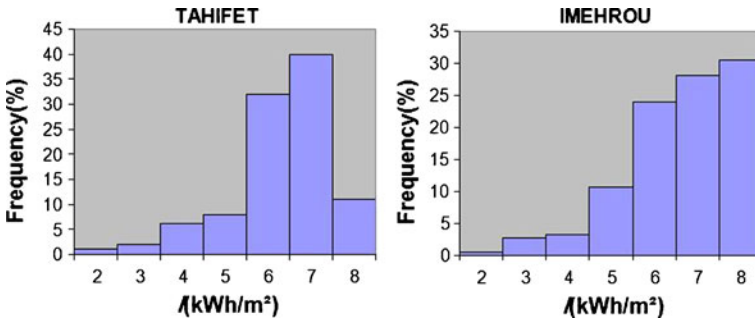


Fig. 3 Distribution of the daily global irradiation over the year

4.3 Implementation

The converted energy series ($E_g(1), E_g(2), \dots, E_g(N)$), ($N = 366$) is divided into m consecutive non-overlapping subseries of length $\tau = N/m$: $E_g((k-1)\tau + 1), E_g((k-1)\tau + 2), \dots, E_g(k\tau)$, $k = 1, 2, \dots, m$. The values of τ in our study range from 10 to $N/2$.

For each subseries the mean:

$$\langle E_g \rangle_{k,\tau} = \frac{1}{\tau} \sum_{t=1}^{\tau} E_g((k-1)\tau + t) \tag{19}$$

and the standard deviation:

$$S_{k,\tau} = \sqrt{\frac{1}{\tau} \sum_{t=1}^{\tau} \{ E_g((k-1)\tau + t) - \langle E_g \rangle_{k,\tau} \}^2} \tag{20}$$

are calculated. Then the stored energy resulted from accumulating the difference between the converted energy and the mean which represents the load consumption is determined:

$$(D_{k,\tau})_t = \sum_{u=1}^t \{ E_g((k-1)\tau + u) - \langle E_g \rangle_{k,\tau} \}, t = 1, 2, \dots, \tau \tag{21}$$

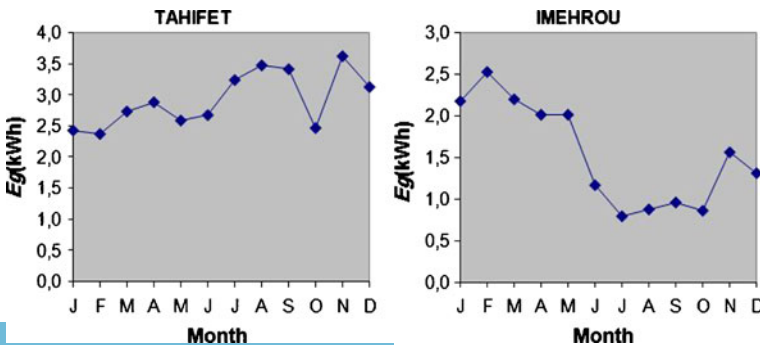


Fig. 4 Monthly mean of daily converted energy

and the range, $R_{k,\tau}$, for the subseries is calculated

$$R_{k,\tau} = \max_{1 \leq t \leq \tau} (D_{k,\tau})_t - \min_{1 \leq t \leq \tau} (D_{k,\tau})_t \tag{22}$$

We finally obtain the rescaled range $(R/S)_\tau$ by averaging $R_{k,\tau}/S_{k,\tau}$ over the m subseries:

$$(R/S)_\tau = \frac{1}{m} \sum_{k=1}^m (R_{k,\tau}/S_{k,\tau}) \tag{23}$$

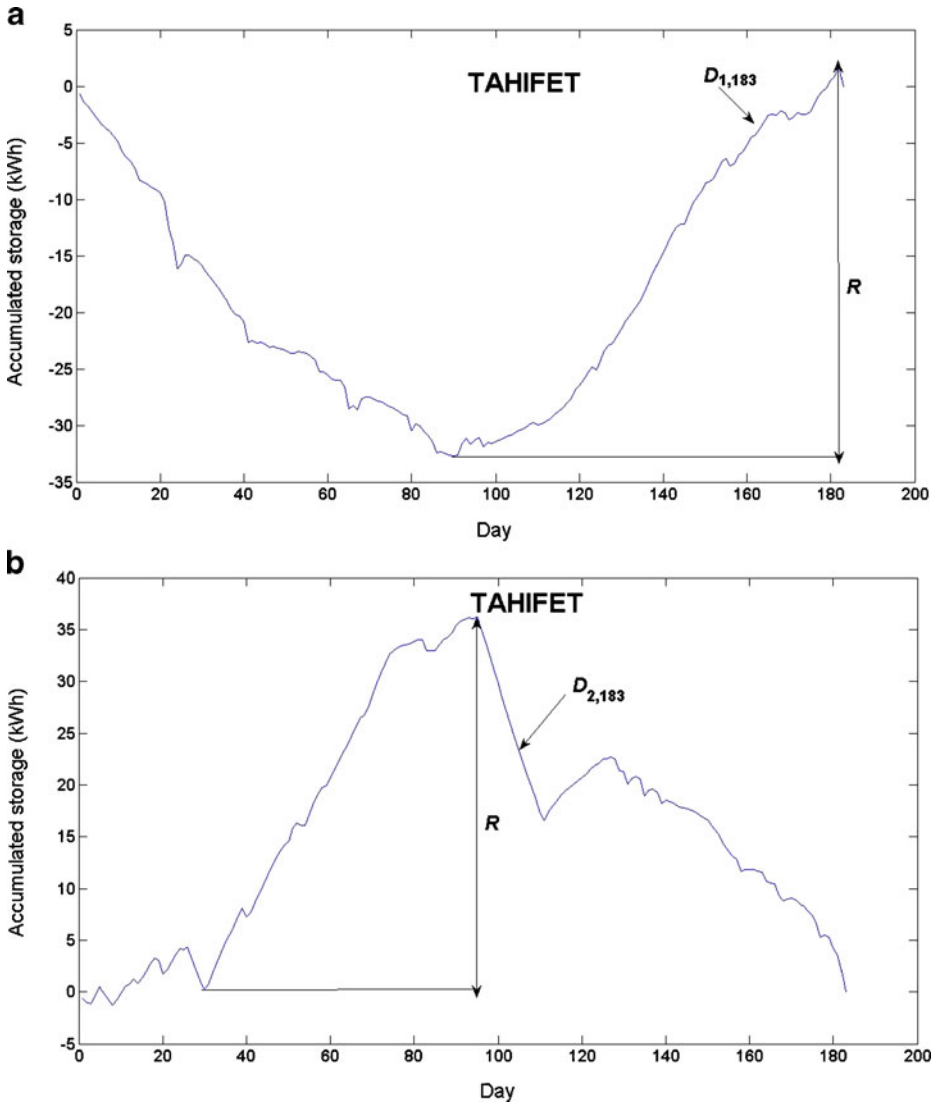


Fig. 5 Accumulated storage $D_{k,\tau}$ of the studied sites for the first 183 days. The range is indicated by R **a** $D_{1,183}$ for Tahifet **b** $D_{2,183}$ for Tahifet **c** $D_{1,183}$ for Imehrou **d** $D_{2,183}$ for Imehrou

5 Results and Discussion

The assessment of our PV storage sizing is carried out using experimental data described above. Thus, for values of τ ranging from 10 to $N/2$, where N is the series size, the accumulated energy ($D_{k,\tau}$) which must be stored in the battery is first computed according to Eq. 21. The resulting curves for the first 183 days are shown in Fig. 5.

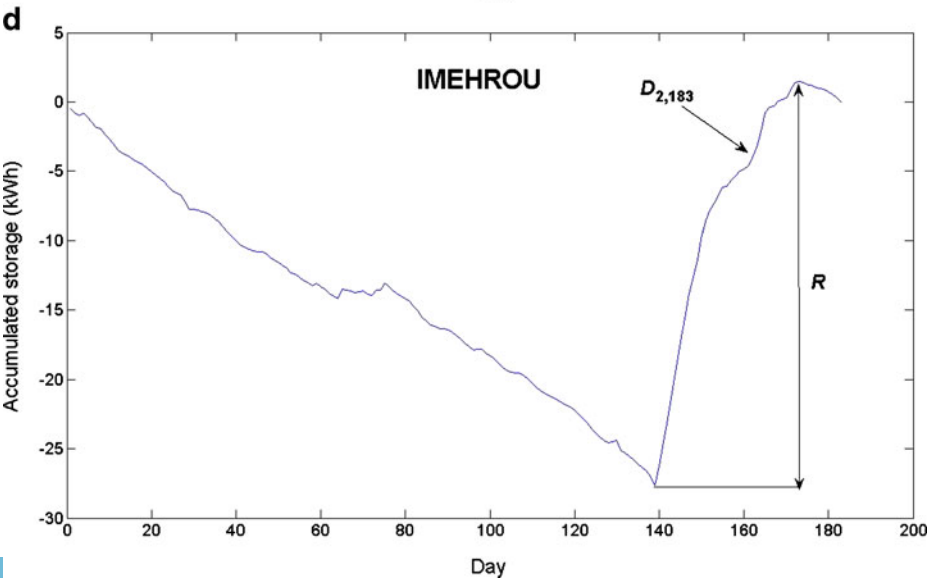
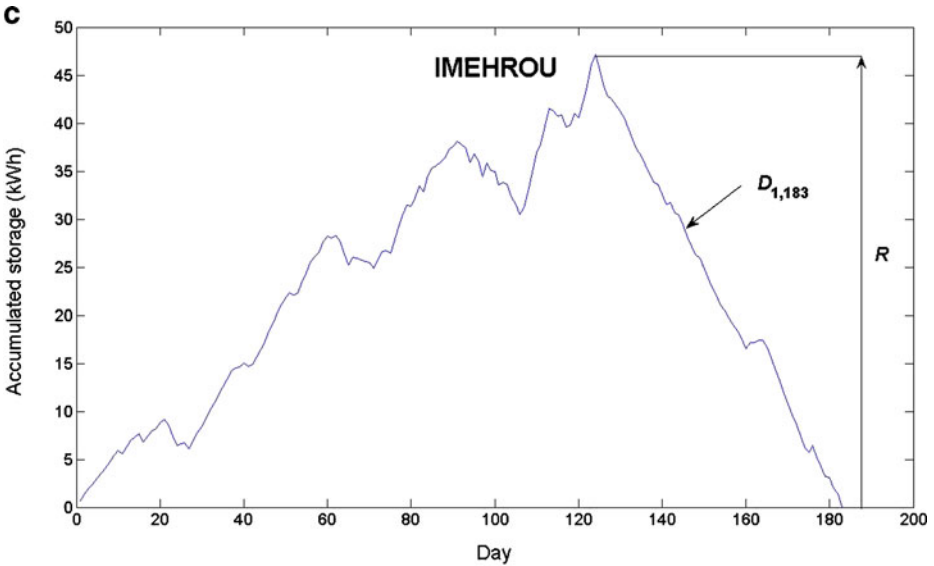


Fig. 5 (continued)

Then, for each τ the range is estimated for the different subseries. The mean values of R for some periods τ are given in Table 1.

One can clearly note that the range depends on the time period τ , in general R increases with increasing τ .

In order to perform the prediction of the PV storage the $(R/S)_\tau$ versus τ plot is developed, this is shown in Fig. 6. It is apparent from the figure that most of $(R/S)_\tau$ points seems to lie along straight line.

A trend line is fitted amongst the $\log(R/S)_\tau$ versus $\log(\tau)$ plot and the coefficient of determination r^2 is computed. This coefficient ranges from 0 to 1, expressed as a percentage, it represents the proportion that can be predicted by the regression line. The values of r^2 found show that 98,5% for Tahifet and 92,2% for Imehrou of the logarithm of the rescaled range is predictable by the regression line, the rescaled range, is then a power function of τ .

In order to perfect the prediction the equation of the trend line is computed for both the sites. The slope coefficients of the equations and the a parameters are given in Table 2.

According to the R/S analysis theory the slope of regression line is identified to the Hurst exponent which is an index of the long memory of the time series. For self-affine time series H is also an index of their roughness which is the role of the fractal dimension. For a curve, D approaches 2 if it is irregular and tends towards 1 if it is regular. Since the Hurst exponent H is related to the fractal dimension D by the relation: $D = 2 - H$, we deduced that high values of H means the curve is smooth and the low values indicate the irregularity of the curve.

Observing the converted energy series used in our study, we found that the corresponding curves are irregular (see Fig. 7), consequently, the corresponding fractal dimension must be high and the Hurst exponent low.

To confirm this, the fractal dimension is calculated for these data using the *Rectangular covering method* we developed and presented in Section 3. The values

Table 1 The range R for different values of τ

τ	R (kWh)	
	Tahifet	Imehrou
10	1.42	1.54
20	2.84	3.14
30	4.17	4.80
40	5.37	5.94
50	7.09	8.57
60	9.03	8.26
70	9.75	11.33
80	12.34	10.50
90	11.52	14.56
100	14.62	13.33
110	16.07	15.76
120	17.05	17.40
130	18.17	10.78
140	20.47	13.28
150	26.12	16.86
160	28.11	20.30
170	31.03	31.45
180	34.11	37.02

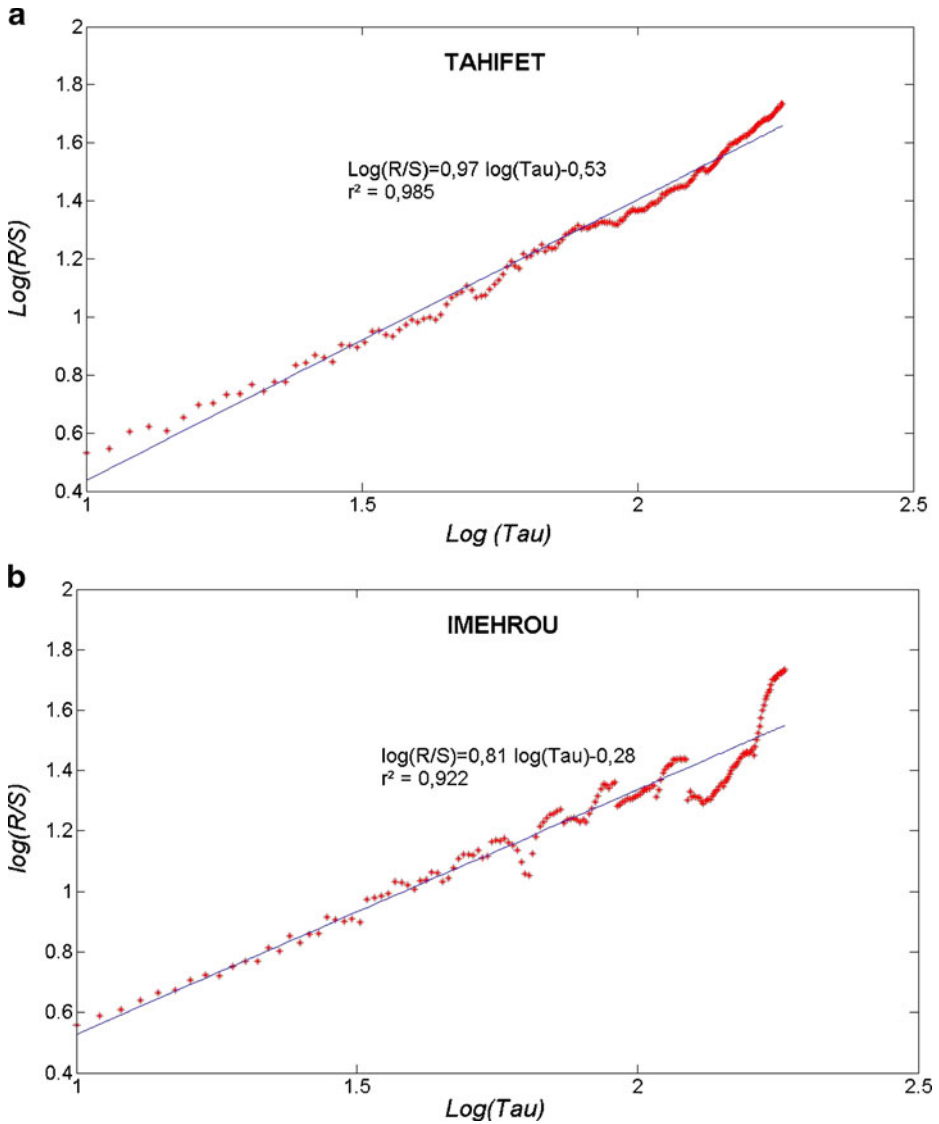


Fig. 6 Log R/S versus Log (τ) Plots **a** Tahifet **b** Imehrou

of the fractal dimension obtained and the corresponding Hurst exponents deduced by Eq. 7 are summarised in Table 3.

The H values found are very far from the slopes of the R/S plot regression lines obtained (0,97 for Tahifet and 0,81 for Imehrou).

Table 2 Parameters of the lines regression equations

Site	Slope coefficient	a
Tahifet	0,97	0,29
Imehrou	0,81	0,52

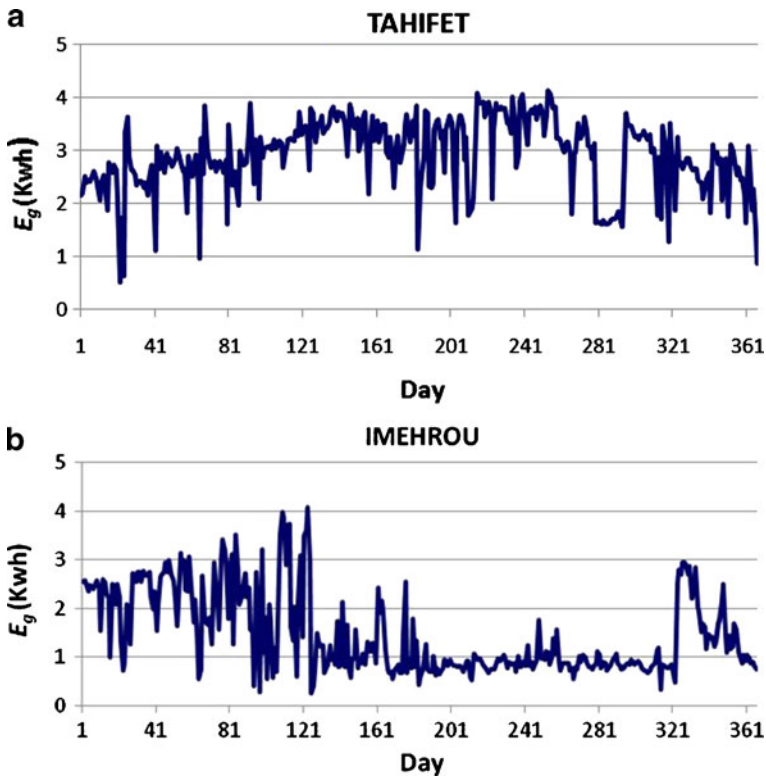


Fig. 7 Yearly evolution of the daily converted energies E_g **a** Tahifet **b** Imehrou

This is can be explained by the non-stationarity of the studied series, since the stationarity of the series is an essential prerequisite for the rescaled range analysis. It is then obvious that the slopes of the fitted lines found are different from the Hurst parameter.

Let’s recall that the purpose of this work is the PV storage prediction and not the Hurst exponent estimation. Therefore, and to avoid any confusion the slopes of the lines we found are noted E instead of H .

Hence, the rescaled range, R/S , for the solar energy converted series studied is described by the following relations where τ is expressed in days:

$$\begin{aligned}
 (R/S)_\tau &= (0.29 \tau)^{0.97} \text{ for Tahifet} \\
 (R/S)_\tau &= (0.52 \tau)^{0.81} \text{ for Imehrou}
 \end{aligned}
 \tag{24}$$

Using the power relations given by Eq. 24 we can predict the storage of the two PV systems studied for any desired period. Table 4 illustrates some predicted values

Table 3 Fractal dimensions and Hurst exponents of the daily converted energies studied

Site	Fractal dimension (D)	Hurst exponent (H)
Tahifet	1,80	0,20
Imehrou	1,81	0,19

Table 4 Predicted values of the R/S and the corresponding R for a period ranging from 1 to 5 years

n (years)	Tahifet		Imehrou	
	R/S	R (kWh)	R/S	R (kWh)
1	92,28	60,90	70,21	49,85
2	180,52	119,14	122,95	87,30
3	267,39	176,48	170,69	121,19
4	353,38	233,23	215,44	152,95
5	438,95	289,70	258,21	183,33

of the adjusted range (R/S) for different time periods n (1 to 5 years) and the corresponding range R which is identified to the maximum size of the PV storage. Note that the medium life duration of PV batteries is 5 years.

Results given in Table 4 show that the proposed approach allowed the prediction of the PV storage of the studied sites starting from a zero initial storage energy. The R values predicted for 5 years are high, to evaluate the autonomy of the solar systems cost, R values have been expressed in number of days of storage (NDS) according to the relation below:

$$NDS = \frac{R}{\langle E_g \rangle} \tag{25}$$

Table 5 gathers the NDS values for the studied sites. Note that NDS is the number of consecutive days where the battery covers consumption needs when there is a deficit in the solar energy production. The NDS values obtained show that for an energy demand equalling the mean of converted energy, a storage of several months is needed to obtain the autonomy of the PV systems, consequently it will be too expensive to set-up such PV installations. Therefore, it is necessary to minimize the size of the storage.

6 Optimisation of the Photovoltaic Storage

Our approach to reduce the photovoltaic storage is based on the fact that the battery supplies the load only when energy produced by PV panels is deficient. Thus, in the accumulated storage function computed by Eq. 21 we consider only the negative values, the storage size R is then determined by Eq. 22 where the maximum and minimum of $(D_{k,\tau})_t$ are calculated for the negative part of the function.

Figure 8 shows the accumulated storage behavior for the first 366 days where the new range R is indicated. The value of this range is found equal to 36 kWh.

Table 5 The photovoltaic systems autonomy

n (years)	NDS (days)	
	Tahifet	Imehrou
1	21	34
2	41	60
3	61	83
4	80	105
5	100	125

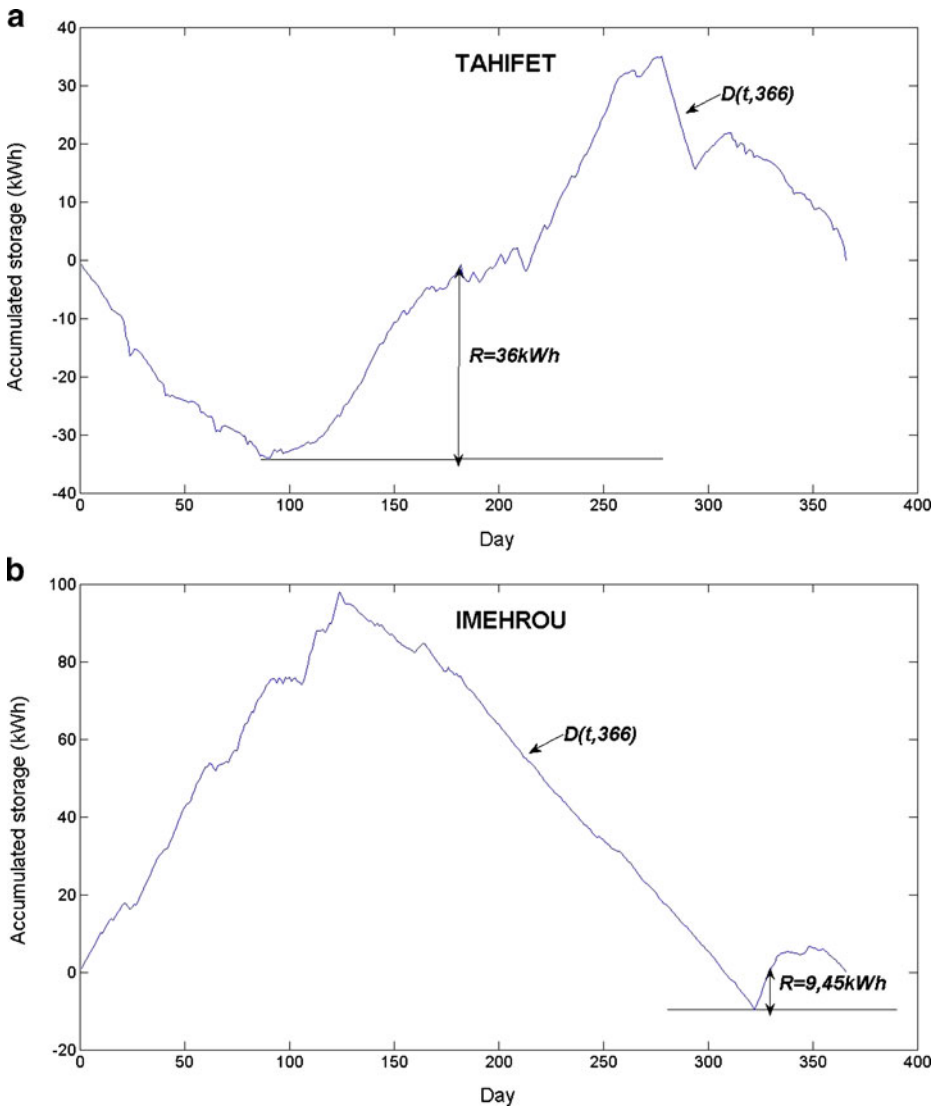


Fig. 8 Accumulated storage $D(t, \tau)$ for the first 366 days **a** Tahifet **b** Imehrou

Table 6 Minimized values of R/S and the corresponding R for a period ranging from 1 to 5 years

n (years)	Tahifet		Imehrou	
	R/S	R (kWh)	R/S	R (kWh)
1	54,54	36,00	13,31	9,45
2	106,83	70,51	23,33	16,57
3	153,31	104,49	32,41	23,01
4	209,27	138,12	40,91	29,05
5	259,84	171,50	49,02	34,80

Table 7 Photovoltaic systems autonomy after the storage size optimization

<i>n</i> (years)	NDS (days)	
	Tahifet	Imehrou
1	13	5
2	25	12
3	36	16
4	48	20
5	59	24

Knowing the value of the new range *R* for one year (366 days) and using the law power:

$$(R/S)_\tau = (a\tau)^E \tag{26}$$

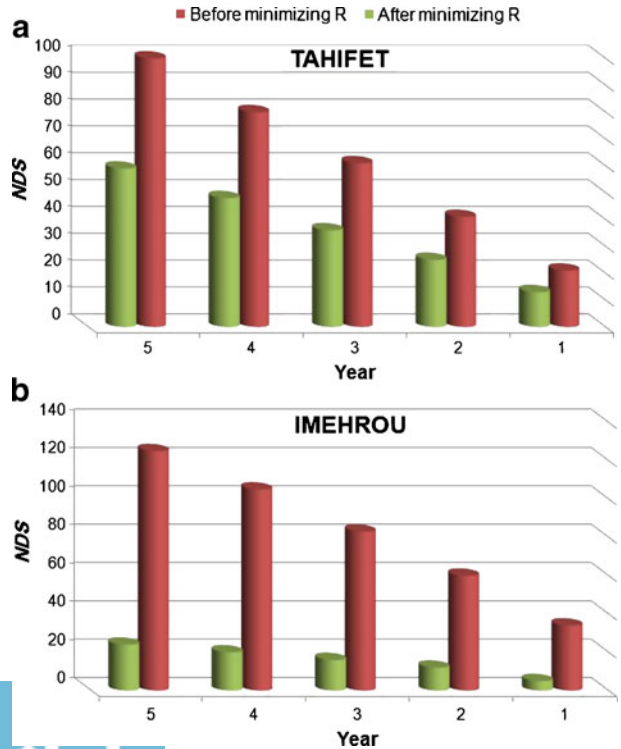
one can predict the new range for the future period according to the equation below:

$$(R/S)_{\tau_2} = (R/S)_{\tau_1} \left(\frac{\tau_2}{\tau_1} \right)^E \tag{27}$$

In this relation τ_1 is the period for which the range *R* has been determined, τ_2 is any future period for which we want to predict the storage. *E* is the slope of the log/log plot of $(R/S)_\tau$ vs. τ already found for the studied sites.

Table 6 gives the new adjusted ranges and the corresponding ranges for time periods *n* ranging from 1 to 5 years. To evaluate the efficiency of the optimized

Fig. 9 Comparison of the PV systems autonomy before and after the storage size optimization **a** Tahifet **b** Imehrou



method proposed, the *NDS* values have been calculated, results obtained are shown in Table 7.

Figure 9 gathers the *NDS* values obtained before and after minimizing the PV storage size with the proposed optimization approach. We remark that the PV storage sizes are been reduced when we apply the optimization method for both the studied sites. The autonomy of the PV Tahifet installation has been reduced by approximately a factor of 1.6, that of the PV system installed in Imehrou by roughly a factor of 5.

7 Conclusion

In this paper, a method for predicting a photovoltaic storage at long-term is presented. It was shown that the rescaled range analysis applied to the solar converted energy data of two Algerian PV installations provides an alternative way to size and predict the PV storage. Results presented here confirm that although the data studied are non-stationary the rescaled range is well described by a power function of the time. A new exponent E different from the Hurst exponent has then been introduced. Results of this work also confirm that the PV storage can be predicted using the power laws established.

A first estimation and prediction of the PV energy storage sufficient to ensure a daily consumption without failure and without loss, leads to values that correspond to several months of storage, which is not economically viable.

To overcome this drawback we proposed an approach to minimize the stock of energy. This approach is based on the fact that the role of the PV storage is to satisfy the energy demand when the photovoltaic energy production is deficient. This differs from the R/S analysis that takes into account in the size of the storage the excess energy produced by solar panels. To eliminate the energy losses we suggest a good sizing of PV panels.

Results of the optimization method show that the proposed approach has led to significant reduction of the PV storage size.

It is important to note that in this work we considered the energy demand to be constant and equal to the mean converted energy. However, the weather conditions and electricity demand are not deterministic in nature but have random behaviour. Therefore, the sizing of battery storage capacity should be based on a stochastic approach which takes into account a real building load profiles. So, the accuracy of the proposed approach can be improved by replacing the constant energy demand by load profiles representing possible realizations of electricity load that could have occurred, these profiles can be generated by an adequate model (see for example [20]).

Preliminary results presented in this paper need further experimentation to validate them by taking a larger data bank and more sites.

References

1. Chapman, R.N.: Development of sizing nomograms for stand-alone photovoltaic/storage systems. *Sol. Energy* **43**, 71–76 (1989)

2. Hadj Arab, A., Ait Idriss, B., Amimeur, R., Lorenzo, E.: Photovoltaic systems sizing for Algeria. *Sol. Energy* **54**, 99–104 (1995)
3. Maafi, A., Delorme, C.: Modélisation à long terme et optimisation du stock d'énergie des installations solaires autonomes. *J. Phys. III France* **6**, 511–527 (1996)
4. Badescu, V.: Time dependent model of a complex PV water pumping system. *Renew. Energy* **28**, 543–560 (2003)
5. Badescu, V.: Dynamic model of a complex system including PV cells, electric battery, electrical motor and water pump. *Energy* **28**, 1165–1181 (2003)
6. Fragaki, A., Markvart, T.: Stand-alone PV system design: results using a new sizing approach. *Renew. Energy* **33**, 162–167 (2008)
7. Tan, C.W., Green, T.C., Hernandez-Aramburo, C.A.: A stochastic method for battery sizing with uninterruptible-power and demand shift capabilities in PV (photovoltaic) systems. *Energy* **35**, 5082–5092 (2010)
8. Hurst, H.E., Black, R.P., Simaika, Y.M.: *Long-term Storage: An Experimental Study*. Constable, London (1965)
9. Mitra, S.K.: Trends in stock prices and range to standard deviation ratio. *Int. J. Bus. Manage* **6**, 223–234 (2011)
10. Feder, J.: *Fractals*. Plenum Press, New York (1988)
11. Zeng, X., Koehl, L., Vasseur, C.: Design and implementation of an estimator of fractal dimension using fuzzy techniques. *Pattern Recogn.* **34**, 151–169 (2001)
12. Tricot, C., Quiniou, J.F., Wehbi, D., Roques-Carmes, C., Dubuc, B.: Evaluation de la dimension fractale d'un graphe. *Rev. Phys.* **23**, 111–124 (1988)
13. Dubuc, B., Quiniou, F., Roques-Carmes, C., Tricot C., Zucker, S.W.: Evaluating the fractal dimension of profiles. *Phys. Rev. A.* **39**, 1500–1512 (1989)
14. Maragos, P., Sun, F.K.: Measuring the fractal dimension of signals: morphological covers and iterative optimization. *IEEE Trans. Signal Process.* **41**, 108–121 (1993)
15. Harrouni, S., Guessoum, A., Maafi, A.: Classification of daily solar irradiation by fractional analysis of 10–min–means of solar irradiance. *Theor. Appl. Climatol.* **80**, 27–36 (2005)
16. Harrouni, S., Guessoum, A.: New method for estimating the time series fractal dimension: application to solar irradiances signals. In: *Solar Energy: New Research*, pp. 277–307. Nova Science Publishers, New York (2006)
17. Harrouni, S.: Fractal classification of typical meteorological days from global solar irradiance: application to five sites of different climates. In: *Modeling Solar Radiation at the Earth's Surface*, pp. 29–54. Springer, Berlin (2008)
18. Harrouni, S., Guessoum, A.: Using fractal dimension to quantify long-range persistence in global solar radiation. *Chaos, Solitons Fractals* **41**, 1520–1530 (2009)
19. Bouligand, G.: Ensembles impropres et nombre dimensionnel. *Bull. Sci. Math.* **II-52**, 320–344, 361–376 (1928)
20. Magnano, L., Boland, J.W.: Generation of synthetic sequences of electricity demand: application in South Australia. *Energy* **32**, 2230–2243 (2007)

Reproduced with permission of the copyright owner. Further reproduction prohibited without permission.